MCPro: A Procedural Method for Topologically Correct Isosurface Extraction Based on Marching Cubes

Julian Stahl[a] and Roberto Grosso[b]

Visual Computing Erlangen, Friedrich-Alexander-Universität Erlangen-Nürnberg, Germany

Keywords: Isosurface Extraction, Marching Cubes, Topological Correctness, Saddle Points, Trilinear Interpolation.

Abstract: In this work, we present an innovative procedural algorithm designed for extracting isosurfaces from scalar data within hexahedral grids. The geometry and the topological features of the intersection of a level set of the trilinear interpolant with the faces and the interior of a reference unit cell are analyzed. Ambiguities are solved without the help of lookup tables, generating a topologically correct triangulation of the level set within the cell that is consistent across cell boundaries. The algorithm is based on constructing and triangulating a polygonal halfedge data structure that includes contours and critical points of the trilinear interpolant. Our algorithm is capable of handling many singular cases that were not solved by previous methods. The efficacy and correctness of the algorithm were tested on a variety of academic and praxis-relevant CT and MRI datasets.

1 INTRODUCTION

Isosurfacing is a technique for visualizing scalar volume data by extracting a surface with a constant isovalue. The surface is often represented as a triangle mesh that can be used for further processing and computations. Marching Cubes (MC) (Lorensen and Cline, 1987) is the most common isosurfacing algorithm because of its simplicity and performance. It computes a triangulation of the surface within discretized cells of the volume based on trilinear interpolation between data points. Especially for computations and mesh processing algorithms, the topology of the extracted mesh is essential. An isosurfacing algorithm that guarantees that the generated meshes are watertight is called topologically consistent. However, a topologically consistent triangulation does not necessarily have the same topology as the trilinear isosurface. If the extracted mesh is homeomorphic to the trilinear interpolant, it is called topologically correct. The original version of Marching Cubes is neither topologically consistent nor correct.

Many improvements have been proposed to make Marching Cubes topologically correct, but some special cases have been often overlooked. Marching Cubes uses predefined triangulations stored in a lookup table and chooses based on 256 cases determined only by the scalar field value on the cell vertices. However, when considering the trilinear interpolant, there is more than one possible triangulation in some cases. These cases are called ambiguous, and many different disambiguation techniques have been proposed. For example, the asymptotic decider (Nielson and Hamann, 1991) will choose the correct branches of the isosurface. The intersection of an isosurface of the trilinear interpolant with an axis-aligned plane is a rectangular hyperbola. The rectangular hyperbola can degenerate into a singular cross, two axis-aligned lines intersecting at a singular vertex for a particular combination of the scalar field values as shown in Figure 1.

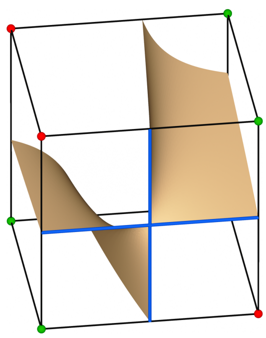

Figure 1: A singular face with a singular point at the intersection of the two axis-aligned lines in blue. Positive and negative corners are marked in green and red.

As we discuss in Section 4, this happens more frequently in medical data where the resolution of

[a] https://orcid.org/0009-0005-7564-9984
[b] https://orcid.org/0000-0001-5965-5325

Stahl, J. and Grosso, R.
MCPro: A Procedural Method for Topologically Correct Isosurface Extraction Based on Marching Cubes.
DOI: 10.5220/0013309800003912

In *Proceedings of the 20th International Joint Conference on Computer Vision, Imaging and Computer Graphics Theory and Applications (VISIGRAPP 2025) - Volume 1: GRAPP, HUCAPP and IVAPP*, pages 331-338
ISBN: 978-989-758-728-3; ISSN: 2184-4321

values is often limited to integers. In such cases, the disambiguation approaches fail to determine the correct topology of the isosurface. Therefore, we propose a new isosurfacing algorithm based on Marching Cubes that generates topologically correct triangulations and can handle singular cases that other methods cannot solve. The triangulations are computed procedurally without using a lookup table, which avoids hand-crafting and storing a large number of possible configurations. The algorithm utilizes simple properties of the isosurface and the trilinear interpolation for robust topology disambiguation.

The contributions of this paper are:

- a lookup table-free, procedural algorithm for topologically correct isosurface extraction
- handling of singular cases
- an open-source implementation (Stahl, 2025)

In Section 2, we discuss related work that focuses on improving the topological properties of Marching Cubes and other isosurfacing methods. In Section 3 the topology of the trilinear interpolant is analyzed and our algorithm is described. We show some results for singular cases and a medical dataset in Section 4 and compare the triangulations generated by our method with the trilinear interpolant. Additionally, we verify our algorithm with a test dataset and discuss non-manifoldness occurring in the trilinear interpolant. Finally, in Section 5, we shortly review and comment on the results of our work.

2 RELATED WORK

The Marching Cubes algorithm was proposed by (Lorensen and Cline, 1987) and has since been improved in many aspects. In this section, we consider advances regarding topological correctness, some of which were summarized by (Newman and Yi, 2006).

There are two kinds of topological ambiguities. Face ambiguity occurs if the two pairs of opposite corners of a face are on different sides of the isosurface. It can lead to holes between adjacent cells if the decision on which corners to connect is inconsistent. One approach to resolve the inconsistency is to exploit only rotational symmetry in the Marching Cubes table (Nielson, 2003), (Nielson et al., 2002). However, a topologically consistent triangulation does not have to be topologically correct; that is homeomorphic to the isosurface of the trilinear interpolant. (Nielson and Hamann, 1991) proposed the asymptotic decider to solve face ambiguity in a topologically correct way.

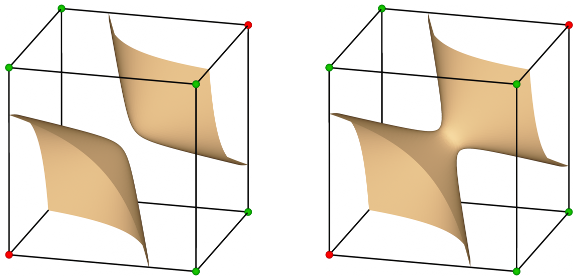

Figure 2: An interior ambiguity: the two diagonally opposed corners may be separated or connected by a tunnel.

(Natarajan, 1994) was the first to describe the problem of interior ambiguity. Here, opposite corners of a cell can be connected by a tunnel, as shown in Figure 2. Natarajan added four subcases to the original 15 cases of Marching Cubes. (Chernyaev, 1996) further extended the Marching Cubes table to include 33 different triangulations. (Etiene et al., 2012) noted that there are cases where the triangulation of MC33 is not topologically correct. (Custodio et al., 2013) proposed the improved version C-MC33. In (Lewiner et al., 2012), an implementation of MC33 using multiple tables to determine subcases was discussed.

Some methods use critical points of the isosurface to determine the topology. (Nielson, 2003) presented an approach with multi-stage decisions that require multiple tables. (Lopes and Brodlie, 2003) uses additional shoulder points and inflection points to increase the geometric accuracy of the triangulation. (Renbo et al., 2005) proposed a table-free variant of Lopes and Brodlie's method that distinguishes cases based on the number of polygons on cell faces and inflection points.

(Custodio et al., 2019) presented an alternative and table-free approach to determine the correct topology inside a cell. They compute connected groups of vertices and create a triangulation based on convex hulls.

(Grosso, 2016) presented a contour-based isosurfacing method that infers the correct topology inside a cell from the number and configurations of isosurface contours on cell faces. In addition, interior points are computed for some cases and used to decide whether a tunnel occurs. The occurrence of singular cases was discussed in (Grosso, 2017).

Other methods rely on subdivisions to resolve topological ambiguities. (Scheidegger et al., 2010) used an adaptive regular subdivision scheme while (Carr and Max, 2010) proposed subdivisions at critical points of the trilinear interpolant.(Hege et al., 1997) proposed an algorithm that uses non-binary classifications of the vertices and assigns them probabilities for interpolation. They also subdivide the cell, followed by a simplification step.

Another algorithm for isosurface computation is Marching Tetrahedra (Treece et al., 1999), based on linear interpolation within the tetrahedra. This results in a different interpolation and therefore isosurface, even when a hexahedral mesh is split into tetrahedra.

Recently, neural isosurfacing methods like Neural Marching Cubes (Chen and Zhang, 2021) or Neural Dual Contouring (Chen et al., 2022) have gained attention. However, these cannot guarantee topological correctness due to their probabilistic nature.

(Etiene et al., 2012) proposed a framework to verify the topological properties of isosurface algorithms, which we will use in Section 4 to test our method.

3 METHOD

Table-based implementations of topologically correct Marching Cubes require hand-crafting many individual triangulations for the different configurations of corner values and possible topologies of a cell. Therefore, we strive towards a universal procedural algorithm based on the properties of the trilinear interpolant. In contrast to previous work, our method includes the topologically correct triangulation of singular cases without increasing in complexity. The following chapter analyzes the isosurface obtained by trilinear interpolation and describes its topological properties. Afterward, an algorithm is presented that leverages these insights to generate a procedural triangulation of the isosurface without relying on lookup tables.

3.1 Topology of Trilinear Interpolation

To analyze the topology of the trilinear interpolation we consider only a single unit cell for simplicity. Marching Cubes assumes the values inside of a cell to be a trilinear interpolation of the corner values $f_0, \dots, f_7$ defined as

$$\begin{aligned} F(u,v,w) = \\ &(1-u)(1-v)(1-w)f_0 + u(1-v)(1-w)f_1 \\ &+(1-u)v(1-w)f_2 + uv(1-w)f_3 \\ &+(1-u)(1-v)wf_4 + u(1-v)wf_5 \\ &+(1-u)vwf_6 + uvwf_7, \end{aligned} \tag{1}$$

where $(u,v,w) \in [0,1]^3$ are the local coordinates of the cell. We assume w.l.o.g. that the isovalue is zero, so the isosurface is described by

$$F(u,v,w) = 0. \tag{2}$$

Positive values are considered to be on the outside of the isosurface, and corners of a cell with a positive or negative value are called positive and negative corners, respectively.

Previous work showed that the topology of the isosurface of a trilinear interpolation can be ambiguous on the faces of the cell and its interior. Firstly, we focus on distinguishing different topological cases of the intersection of the isosurface with a face. In the following, we consider the face $w = 0$ with corner values f_0, f_1, f_2, f_3. The restriction of Equation (1) to the plane defined by this face is the bilinear interpolation

$$\begin{aligned} F_{w=0}(u,v) = (1-v)((1-u)f_0 + uf_1) \\ +v\ ((1-u)f_2 + uf_3), \end{aligned} \tag{3}$$

which can be written in normal form as

$$F_{w=0}(u,v) = \alpha + \eta(u-u_0)(v-v_0) \tag{4}$$

with

$$\eta = f_0 - f_1 - f_2 + f_3 \tag{5}$$

$$\alpha = \frac{f_0 f_3 - f_1 f_2}{\eta} \tag{6}$$

$$u_0 = \frac{f_0 - f_2}{\eta},\ v_0 = \frac{f_0 - f_1}{\eta}. \tag{7}$$

This form shows that the intersection of the isosurface with a plane is generally a hyperbola as shown in Figure 3a with the asymptotes $u = u_0$ and $v = v_0$ when $\alpha \neq 0$ and $\eta \neq 0$. However, Equation (4) can degenerate and lead to three other topological cases on the face that are shown in Figure 3. If $\alpha = 0$ and $\eta \neq 0$, the hyperbola collapses to the two lines $u = u_0$ and $v = v_0$ in Figure 3b that meet at the center of the asymptotes (u_0, v_0). We call a face with this topology a singular face and the point (u_0, v_0) a singular point on the face. This point is not necessarily singular in three dimensions depending on the incident cells.

If $\eta = 0$ Equation (4) is no longer defined. Instead, the bilinear interpolation from Equation (3) degenerates to the linear interpolation

$$F_{w=0}(u,v) = f_0 + u(f_1 - f_0) + v(f_2 - f_0), \tag{8}$$

where the solution to $F_{w=0}(u,v) = 0$ is either a single straight line visualized in Figure 3c or in the case $f_0 = f_1 = f_2 = f_3 = 0$ the solution is the whole plane $w = 0$ shown in Figure 3d.

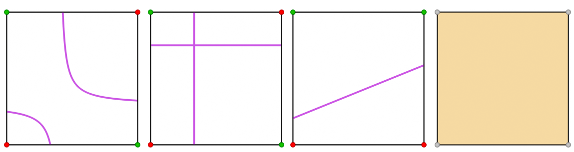

(a) hyperbola (b) cross (c) single line (d) plane

Figure 3: The topologies of the isosurface on a face.

The cases where the intersection of the isosurface with a face is a single line or the whole plane cannot be ambiguous. However, the hyperbolic and singular cases have an ambiguous topology because they consist of two branches of the isosurface. From the signs of the values $f_0,\ldots,f_3$, it cannot be determined how the two branches are oriented. In the singular case, the two branches meet at the center of the asymptotes, but if we move in the direction orthogonal to the surface, the two branches will separate or merge, see Figure 10. The correct topology is defined by the limit when the face is approached from the cell's interior.

After resolving face ambiguities, we now analyze interior ambiguities of the trilinear interpolant. Interior ambiguities can even occur if no faces are ambiguous. The isosurface can be described in parametric form by solving Equation (2) for one of u,v, or w, e.g.

$$w(u,v) = \frac{auv+bu+cv+d}{euv+fu+gv+h}, \tag{9}$$

where $a,\ldots,h$ depend on the values at the cell corners $f_0,\ldots,f_7$. We look at the critical points' existence and positions to determine the topology of the isosurface. Between critical points and the cell's boundaries, the surface is monotonic. The surface defined by $w(u,v)$ has up to two critical points that satisfy

$$\frac{\partial w(u,v)}{\partial u} = \frac{\partial w(u,v)}{\partial v} = 0. \tag{10}$$

These critical points are saddle points of the isosurface because the determinant of the Hessian is negative at the critical points, so minima and maxima do not exist. The same holds for $u(v,w)$ and $v(u,w)$, resulting in up to six critical points of the isosurface. Because the partial derivatives in two directions are zero, the saddle points lie on the intersections of two axis-aligned lines that are part of the isosurface, as shown in Figure 4a.

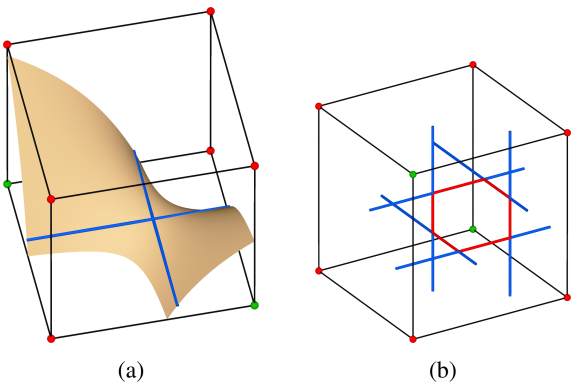

Figure 4: (a) A saddle point is located at the intersection of two axis-aligned anchor lines shown in blue. (b) The inner hexagon marked in red consists of six critical points on the anchor lines forming a cuboid.

We call these axis-aligned lines with constant value *anchor* lines. There can be at most six of these anchor lines. The saddle points are the same ones computed by (Grosso, 2016) by solving three quadratic equations. The advantage of the formulation in Equation (10) is that it is not based on the intersection of the isosurface with cell faces that can degenerate to the singular case. If all six critical points exist, they form six corners of a cuboid, where two diagonally opposite corners are missing. This structure is called DeVella's Necklace (Nielson, 2003) or Inner Hexagon (Grosso, 2016) and is visualized by the red lines in Figure 4b. The case of two crossing lines, Figure 3b, occurs precisely in the case where one or more vertices of the inner hexagon lie on a face of the cell.

3.2 Triangulation Algorithm

Due to the high number of possible combinations of cell corner values, face ambiguities, interior ambiguities, and singularities, storing all potential cases of triangulations in tables is infeasible. The triangulation is therefore generated procedurally based on properties of the trilinear interpolation inside a cell. All configurations are processed similarly without relying on many execution paths for individual edge cases. For example, cases that contain cell corners with exactly the isovalue do not require a large increase of handcrafted triangulations as proposed by (Raman and Wenger, 2008). The algorithm is split into four stages that analyze features of increasing dimensionality of the grid. This enables efficient parallelization and reduces duplicate computations. Our algorithm creates the triangulation based on contours on the faces and interior of a cell. The isosurface is represented by oriented segments stored in a halfedge data structure that allows efficient insertion and updates.

The first three stages of the algorithm are iterating all cell edges of the grid, then the faces, and lastly, the cells. While the edges are considered, new vertices are created. When the faces are analyzed, if the face is singular, a new vertex on the face is created, and the vertices are connected to line segments. While iterating the cells in the third stage, a halfedge data structure is created by connecting the segments to form contours, interior vertices are added, and the interior structure is connected to the contours. In the final step, the halfedge data structure is triangulated to create a mesh. In the following, the principal steps of the algorithm are explained in more detail.

Firstly, all edges are iterated and checked for an intersection with the isosurface. If the values at the endpoints of an edge are on different sides of the isosurface, a new vertex is created at the position determined by linear interpolation. If both endpoints of an edge lie on the isosurface, they are added to the list of vertices, and no interpolation is performed. Otherwise, the edge does not intersect the isosurface and can be ignored.

Next, the faces are considered. The intersection of the isosurface with a plane can have four different mathematic descriptions that are distinguished by the asymptotic decider in Equation (6). Based on these different topologies, the vertices on a face are connected to segments. Therefore, each face is divided into quadrants based on the center of the asymptotes given by Equation (7). The vertices on the face are sorted into their respective quadrants. The non-empty quadrants must contain two vertices that are connected by a segment. The singular cases can be solved similarly by connecting all vertices on the cell's edges to the central, singular vertex on the face.

Because the segments are later converted to halfedges, they must be correctly oriented. Each segment has a tangential and a normal direction, where the normal is on the left side of the tangent. Since we defined positive values as outside the isosurface, the normal of the line segments should always point towards a positive corner of the face. The orientation of the segment is computed based on its normal direction and the sign of a corner in the same quadrant like in Figure 5a. For singular faces, the normal of the face at the asymptotic center is also used to decide how the four segments are connected. Connected segments must rotate counter-clockwise for a face normal facing outwards as shown in Figure 5b. Repeating this procedure for all faces leads to the segments in Figure 5c that represent the intersection of the isosurface with the faces of a cell.

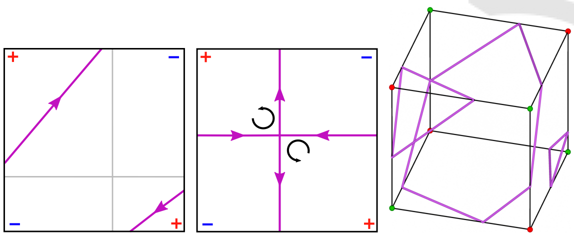

(a) hyperbolic face (b) singular face (c) outer contours

Figure 5: The segments on a face are connected and oriented based on corner values and the face normal to form contours.

Finally, the segments on the faces are connected to form contours on the cell faces, and the topology of the isosurface inside the cell is evaluated. The mesh inside of a cell is represented by a local halfedge data structure. The segments generated on the faces of the cell are inserted and pointers to the next and previous halfedges are stored. Then, two opposite critical points are computed by solving the system of equations (10). The remaining four points of the inner hexagon shown in Figure 4b are inferred by combining the coordinates of the two known solutions. The anchor lines and the hexagon shown in Subsection 3.1 form a skeleton inside the cell that is used to determine the triangulation. All critical points inside the cell are added to the list of vertices. The critical points that lie on the face coincide with the points already calculated during the face iteration and are therefore not added to the list. The intersections of an anchor line with the faces of the cell will always lie on a contour of the exact, trilinear isosurface as can be seen in Figure 6a. To connect the inner hexagon with the outer contours, segments are created from every critical point to the outer vertices according to the skeleton of anchor lines. However, the outer end of an anchor line generally does not coincide with a contour vertex. Thus, the vertex that corresponds to the intersected contour and is closest to the intersection point with the face is chosen instead. This is repeated for all critical points. Additionally, the segments of the inner hexagon are added to complete the inner skeleton of halfedges shown in Figure 6b. The connectivity of halfedges at the inner vertices is decided by choosing the surface normal to face outward according to the interpolated gradient of the function values at that point. The outer contour is split at intersected vertices and is newly connected to and from the inner vertices. This way, the created halfedge data structure describes a polygonal mesh of the isosurface.

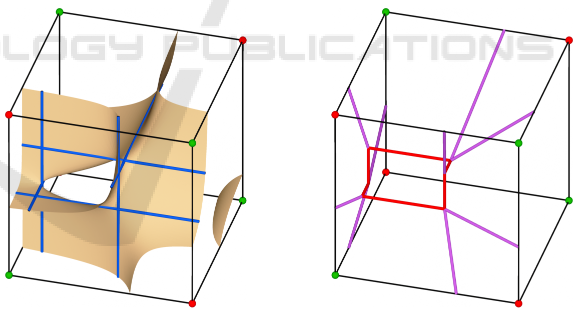

(a) (b)

Figure 6: (a) The intersection of the anchor lines with the faces of the cell is always on the contour of the isosurface. (b) The contours of the isosurface inside a cell based on the skeleton of anchor lines.

Because the isosurface is monotonic between critical points, its topology is equivalent to a disk's. The resulting polygons described by the halfedge data structure can therefore be triangulated as disks. This is done by iteratively replacing two incident halfedges with the spanned triangle and inserting the third side as a new halfedge. The resulting mesh can be output as an indexed face set or a global halfedge data structure.

This formulation inherently solves many configu-

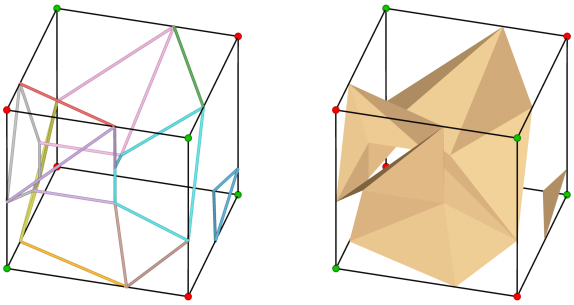

Figure 7: The halfedge data structure represents the surface as polygons shown in different colors on the left. The polygons are triangulated to create the final mesh on the right.

rations that previous methods could only solve based on some decision criteria for the correct topology. For example, the normals of neighboring saddle points decide whether a tunnel or disc is created for MC case 13 because the halfedges will be oriented differently. From there, the same triangulation algorithm creates the correct meshes for both topologies instead of needing to define an explicit case distinction.

4 RESULTS

In this section, we present some results of our new triangulation algorithm, test the method on real-world datasets, and show some singular cases of implicitly defined surfaces for the trilinear interpolant that are non-manifold. For comparison purposes we use the MC33 implementation in the scikit library, (van der Walt et al., 2014).

In contrast to previous work, we focused on the cases where the intersection of the isosurface with a cell face is a degenerated hyperbola. Our table-free method generates topologically correct triangulations compared to the trilinear interpolant. Some examples of such cases on one or multiple faces can be seen in Figure 8. A reference for the exact trilinear isosurface is obtained by subdividing each cell at least 100 times and computing the isosurface within the subcells. Tunnels in the isosurface are correctly represented in the mesh created by our method, even for the singular cases where one or more saddle points lie on the faces of the cell. MC33 can not produce a topologically correct mesh for these cases. For the middle case in Figure 8 with three singular faces next to each other, MC33 creates a tunnel with triangles on the cell faces, leading to an incorrect non-manifoldness when connected to the neighboring cells. Our use of a halfedge data structure prevents this by describing the face neighborhood with opposite halfedges.

We verified our algorithm with the test datasets provided by (Etiene et al., 2012). The datasets contain

Table 1: The number of mesh elements of the human skull (isovalue 950) created by our method, MC33, and MC.

Method	Ours	MC33	MC
Vertices	1213089	1102349	1093007
Triangles	2434920	2219708	2212832

10000 single-cell examples, and 10000 closed surfaces together with precomputed topological invariants. To compare the topology of the meshes generated by our method to the trilinear interpolant, we use Betti numbers b_i (Konkle et al., 2003). Only b_0, b_1, and b_2 can be non-zero in three-dimensional space. Here, b_0 describes the number of connected components. b_1 counts the one-dimensional holes of an object and can be computed as $b_1 = 2g$, where g is the genus of the surface (Theisel, 2002). The number b_2 represents the regions of space enclosed by the surface. We additionally used the Euler characteristic $\chi = V - E + F$ as a topological invariant for comparisons. Our method generates isosurfaces with the correct topology in all 20000 examples provided by the test datasets. Note that the test datasets did not contain any singular faces.

We used our algorithm to compute the isosurface from some real-world datasets of a human skull, a mecanix, a Porsche, and a carp, as shown in Figure 9. CT and MRI datasets contain only 16-bit integer data values, which increases the probability for singular faces and non-manifold cases. We analyzed 22 datasets of which all but one contain singular faces and therefore require special handling of these cases. Our algorithm produces a more detailed mesh because critical points are included in the triangulation. Therefore, the number of vertices and triangles increases compared to MC33. As Table 1 shows for the example of the human skull dataset, our method generates approximately 10 % more vertices and faces than the standard Marching Cubes and the MC33 algorithms.

We now look at non-manifoldness occurring in the trilinear interpolant. The face of a cell whose intersection with the isosurface is a degenerated hyperbola contains a vertex on the face. Although the vertex is singular on the face, it can be part of a continuous surface through the two incident cells where the vertex is not singular in three dimensions. In Figure 10, we see on the left that the cross lies on a single branch of the isosurface, and thus, the singular point is manifold in 3D. On the other side, on the right, we see two branches of the isosurface touch at the singular point. The singular point corresponds to a singularity of the implicit surface, creating a non-manifold vertex.

The previous example shows that the trilinear interpolant can be singular on faces, edges, and corners, for which the topologically correct triangulation

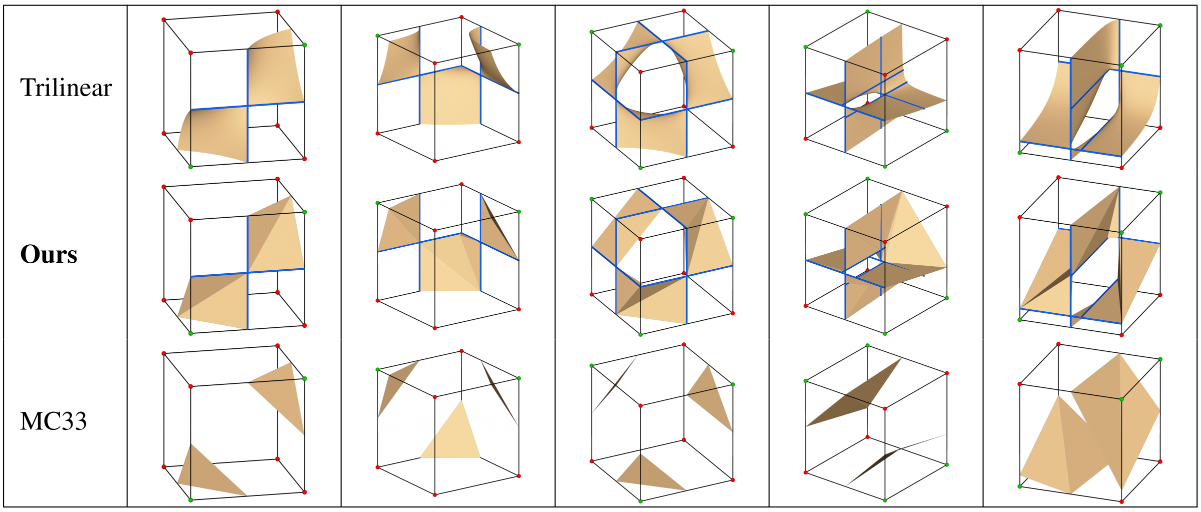

Figure 8: The triangulations created by subdividing and interpolating the grid values, our method, and MC33 for cases with at least one degenerated hyperbola.

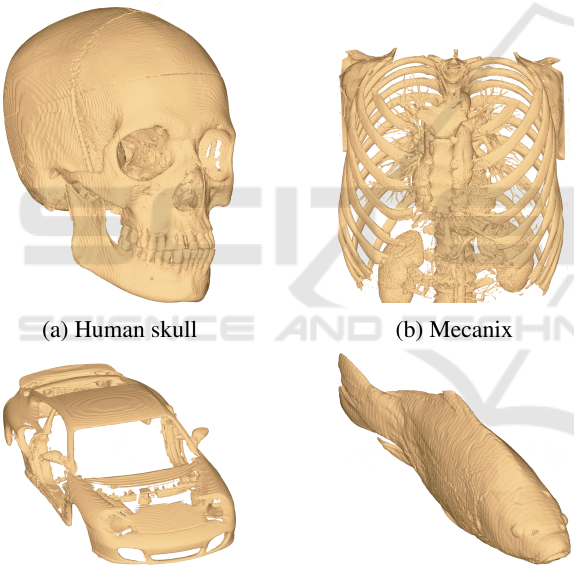

(a) Human skull (b) Mecanix

(c) Porsche (d) Carp

Figure 9: Meshes generated with our method from a selection of real-world datasets.

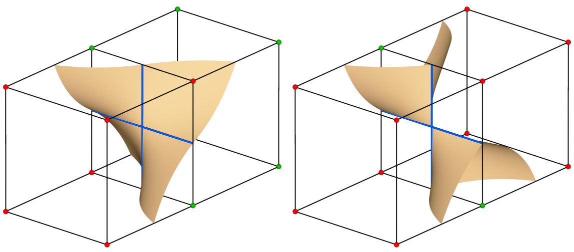

Figure 10: Two cells that share a singular face can either result in a continuous surface (left) or a singular surface with a non-manifold vertex (right).

is non-manifold. As seen in Figure 11, Singularity can also occur within a cell. A singular point occurs if all six saddle points coincide and the tunnel collapses to a single point in space. In this case, the isosurface and the topologically correct triangulation are non-manifold. The case of an isosurface, which is non-manifold along an edge, occurs if the scalar values of the cell vertices are symmetric in such a way that an axis-aligned plane is part of the isosurface.

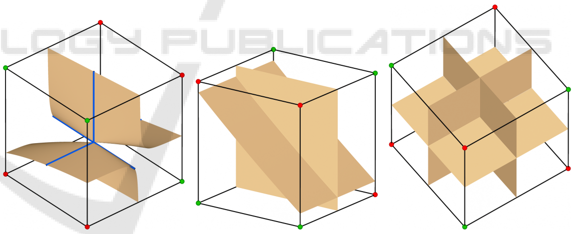

Figure 11: Non-manifold vertices and edges can occur in the trilinear interpolant.

The geometric accuracy of the triangulation of the isosurface within a cell can be improved by edge flips for some cases where the three-dimensional shape of the polygons that make up the isosurface is not optimal. The topologically correct triangulation of cases containing non-manifold edges, such as in Figure 11, will be the subject of future work.

5 CONCLUSIONS

We presented an isosurface method that generates meshes topologically equivalent to the isosurface of the trilinear interpolation of a scalar field. The method does not rely on lookup tables like many previous variants of Marching Cubes. Instead, it generates the triangulation in a procedural algorithm based on a local halfedge data structure. The correct topology is determined by the contours on the cell faces and the configuration of critical points inside the cell. Compared to previous methods, our approach generates topologically correct triangulations for cases where the intersection of the trilinear interpolant and a cell face is not hyperbolic but degenerates into two crossing lines. Our method creates a more detailed mesh by making use of critical points of the surface. We showed that an isosurface based on trilinear interpolation can be non-manifold both inside of a cell and on the boundary between cells, so a topologically correct triangulation should include these non-manifold features.

ACKNOWLEDGEMENTS

This work was funded by the Deutsche Forschungsgemeinschaft (DFG, German Research Foundation) – 502500606.

REFERENCES

Carr, H. and Max, N. (2010). Subdivision Analysis of the Trilinear Interpolant. *IEEE Transactions on Visualization and Computer Graphics*, 16(4):533–547.

Chen, Z., Tagliasacchi, A., Funkhouser, T., and Zhang, H. (2022). Neural dual contouring. *ACM Trans. Graph.*, 41(4):104:1–104:13.

Chen, Z. and Zhang, H. (2021). Neural marching cubes. *ACM Trans. Graph.*, 40(6):251:1–251:15.

Chernyaev, E. (1996). Marching Cubes 33: Construction of Topologically Correct Isosurfaces. *No. CERN-CN-95-17*.

Custodio, L., Etiene, T., Pesco, S., and Silva, C. (2013). Practical considerations on Marching Cubes 33 topological correctness. *Computers & Graphics*, 37(7):840–850.

Custodio, L., Pesco, S., and Silva, C. (2019). An extended triangulation to the Marching Cubes 33 algorithm. *Journal of the Brazilian Computer Society*, 25(1):6.

Etiene, T., Nonato, L. G., Scheidegger, C., Tienry, J., Peters, T. J., Pascucci, V., Kirby, R. M., and Silva, C. T. (2012). Topology Verification for Isosurface Extraction. *IEEE Transactions on Visualization and Computer Graphics*, 18(6):952–965.

Grosso, R. (2016). Construction of Topologically Correct and Manifold Isosurfaces. *Computer Graphics Forum*, 35(5):187–196.

Grosso, R. (2017). An asymptotic decider for robust and topologically correct triangulation of isosurfaces: topologically correct isosurfaces. *Proceedings of the Computer Graphics International Conference*, pages 1–5.

Hege, H.-C., Stalling, D., Seebass, M., and Zöckler, M. (1997). A generalized marching cubes algorithm based on non-binary classifications. *SC-97-05*.

Konkle, S. F., Moran, P. J., Hamann, B., and Joy, K. I. (2003). Fast methods for computing isosurface topology with betti numbers. In *Data Visualization: The State of the Art*, pages 363–375.

Lewiner, T., Lopes, H., Vieira, A., and Tavares, G. (2012). Efficient Implementation of Marching Cubes' Cases with Topological Guarantees. *Journal of Graphics Tools*, 8.

Lopes, A. and Brodlie, K. (2003). Improving the robustness and accuracy of the marching cubes algorithm for isosurfacing. *IEEE Transactions on Visualization and Computer Graphics*, 9(1):16–29.

Lorensen, W. E. and Cline, H. E. (1987). Marching cubes: A high resolution 3D surface construction algorithm. In *Proceedings of the 14th annual conference on Computer graphics and interactive techniques*, SIGGRAPH '87, pages 163–169.

Natarajan, B. K. (1994). On generating topologically consistent isosurfaces from uniform samples. *The Visual Computer*, 11(1):52–62.

Newman, T. S. and Yi, H. (2006). A survey of the marching cubes algorithm. *Computers & Graphics*, 30(5):854–879.

Nielson, G. (2003). On Marching Cubes. *IEEE Transactions on Visualization and Computer Graphics*, 9:283–297.

Nielson, G. and Hamann, B. (1991). The asymptotic decider: resolving the ambiguity in marching cubes. In *Proceeding Visualization '91*, pages 83–91.

Nielson, G., Huang, A., and Sylvester, S. (2002). Approximating normals for marching cubes applied to locally supported isosurfaces. In *IEEE Visualization, 2002. VIS 2002.*, pages 459–466.

Raman, S. and Wenger, R. (2008). Quality Isosurface Mesh Generation Using an Extended Marching Cubes Lookup Table. *Computer Graphics Forum*, 27(3):791–798.

Renbo, X., Weijun, L., and Yuechao, W. (2005). A Robust and Topological Correct Marching Cube Algorithm Without Look-Up Table. In *The Fifth International Conference on Computer and Information Technology (CIT'05)*, pages 565–569.

Scheidegger, C., Etiene, T., Nonato, L. G., and Silva, C. T. (2010). Edge Flows: Stratified Morse Theory for Simple, Correct Isosurface Extraction. *SCI Institute, University of Utah, SCI Technical Report UUSCI-2010-002*.

Stahl, J. (2025). MCPro [Software]. *Github. https://github.com/JulyCode/MCPro*.

Theisel, H. (2002). Exact Isosurfaces for Marching Cubes. *Computer Graphics Forum*, 21(1):19–32.

Treece, G. M., Prager, R. W., and Gee, A. H. (1999). Regularised marching tetrahedra: improved iso-surface extraction. *Computers & Graphics*, 23(4):583–598.

van der Walt, S., Schönberger, J. L., Nunez-Iglesias, J., Boulogne, F., Warner, J. D., Yager, N., Gouillart, E., Yu, T., and the scikit-image contributors (2014). scikit-image: image processing in Python. *PeerJ*, 2:e453.